Optica Applicata, Vol. XI, No. 1, 1981

Spectrum transfer of one-dimensional periodic object in optical systems with nonuniformly slit-like aperture*

Anna Magiera, Marek Zając

Institute of Physics, Technical University of Wrocław, Wybrzeże Wyspiańskiego 27, 50-372 Wrocław, Poland.

Intensity distributions in the diffraction pattern generated by one-dimensional periodic objects have been determined. The dependence of the diffraction pattern upon the luminance distribution in the light source and the object structure has been numerically examined. The numerical calculations have been carried out for all combinations of source luminance distribution, object width and spatial frequency of the structure.

1. Introduction

Up to date a number of works concerning the imaging of periodic objects have been published. In particular, the images of truncated sinusoidal and rectangular periodic structures in the systems with slit aperture were examined in papers [1, 2]. The case of truncated one-dimensional periodic structure was examined in [3]. The contrast in periodic object imaging in partially coherent systems was the subject of the work [4]. In the paper [5] the influence of parabolic apodization on the contrast of imaging of truncated periodic triangle and rectangular structures was examined. In all the papers mentioned the imaging was tested in the image plane while the objects under test were simple periodic structures.

In the case of more complex objects the information quantity contained in the object exceeds often the analysing capabilities of the receptor. In order to extract definite information about the object the technique of optical filtering is often used; it consist essentially in manipulating on the object spatial frequency spectrum. To perform this manipulation in a reasonable way the knowledge of the properties of the object spectrum (to be manipulated) may be very helpful. Therefore, this work is devoted to investigations of the object spectrum of truncated periodic objects.

---

* This work was carried on under the Research Project M.R. I.5.

2. General relations

A typical system for visualization of Fourier spectrum of an object is shown in fig. 1. The light source is located in the plane P_0. An objective, located in the plane P_1, creates a collimating system for the light emitted

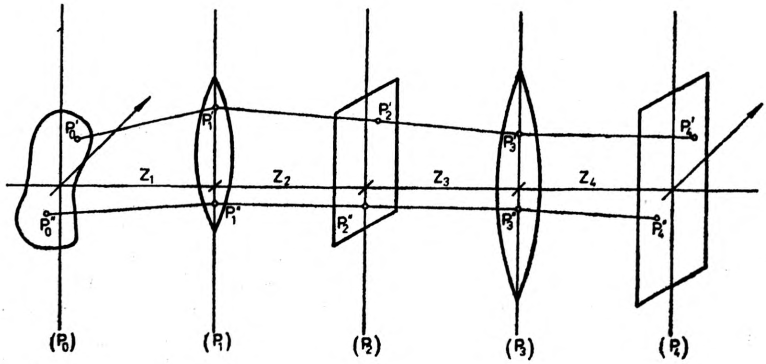

Fig. 1. Optical system:
P_0 – plane of the light source S, P_1 – plane of the collimator, P_2 – plane of the object, P_3 – Fourier transforming lens, P_4 – Fourier plane

by the source. The object of amplitude transmittance A is placed in the plane P_2. Another objective, positioned in the plane P_3, realizes a diffraction image of the object in the plane P_4. The propagation of the mutual coherence function from the plane P_0 to the plane P_1 is described by the well-known integral [6]:

$$\Gamma_1(P_1', P_1'') = \frac{\exp\left[\frac{ik}{2z_1}(P_1'^2 - P_1''^2)\right]}{\lambda z_1} \iint \Gamma(P_0', P_0'')\exp\left[\frac{ik}{2z_1}(P_0'^2 - P_0''^2)\right]$$
$$\times\exp\left[-\frac{ik}{z_1}(P_0'P_1' - P_0''P_1'')\right] dP_0' dP_0''. \tag{1}$$

In the plane P_1 the incident light distribution is modulated by the lens transmittance. When assuming that the lens is thin, infinitely extended* and aberration-free, we obtain behind the lens

$$\Gamma_1'(P_1', P_1'') = \Gamma_1(P_1', P_1'')\exp\left[-\frac{ik}{2z_1}(P_1'^2 - P_1''^2)\right]. \tag{2}$$

* The lens size restriction may be taken into consideration by multiplying the lens transmittance by the respective aperture function. The lens aberrations were not taken into account as our goal is to compare the action of optical systems with and without amplitude apodizers. As shown in [7] the optical systems designed to work with apodizers must be well-corrected.

The propagation from the plane P_1 to the plane P_2 is described by the dependence

$$\Gamma_2(P_2', P_2'') = \frac{1}{\lambda z_2} \exp\left[\frac{ik}{2z_2}(P_2'^2 - P_2''^2)\right] \iint \Gamma_1'(P_1', P_1'')$$
$$\times \exp\left[\frac{ik}{2z_2}(P_1'^2 - P_1''^2)\right]$$
$$\times \exp\left[-\frac{ik}{z_2}(P_1'P_2' - P_1''P_2'')\right] dP_1' dP_1''. \tag{3}$$

Immediately behind the object plane P_2 we have

$$\Gamma_2'(P_2', P_2'') = \Gamma_2(P_2', P_2'') A(P_2') A^*(P_2''). \tag{4}$$

The propagation from the object plane P_2 to the imaging lens plane P_3 is expressed as follows:

$$\Gamma_3(P_3', P_3'') = \frac{1}{\lambda z_3} \exp\left[\frac{ik}{2z_3}(P_3'^2 - P_3''^2)\right] \iint \Gamma_2'(P_2', P_2'')$$
$$\times \exp\left[\frac{ik}{2z_3}(P_2'^2 - P_2''^2)\right]$$
$$\times \exp\left[-\frac{ik}{z_3}(P_2'P_3' - P_2''P_3'')\right] dP_2' dP_2''. \tag{5}$$

Behind the lens it holds

$$\Gamma_3'(P_3', P_3'') = \Gamma_3(P_3', P_3'') \exp\left[-\frac{ik}{2z_3}(P_3'^2 - P_3''^2)\right]. \tag{6}$$

The propagation of the mutual coherence function from the plane P_3 to P_4 takes the form

$$\Gamma_4(P_4', P_4'') = \frac{1}{\lambda z_4} \exp\left[\frac{ik}{2z_4}(P_4'^2 - P_4''^2)\right] \iint \Gamma'(P_3', P_3'')$$
$$\times \exp\left[\frac{ik}{2z_4}(P_3'^2 - P_3''^2)\right]$$
$$\times \exp\left[-\frac{ik}{z_4}(P_3'P_4' - P_3''P_4'')\right] dP_3' dP_3''. \tag{7}$$

Assuming that $z_1 = z_2 = z_3 = z_4 = f$ the mutual coherence function takes the form

$$\Gamma_4(P_4', P_4'') = \frac{1}{\lambda^8 f^8} \exp\left[\frac{ik}{2f}(P_4'^2 - P_4''^2)\right] \int_1 \ldots \int_8 \Gamma(P_0', P_0'') A(P_2') A^*(P_2'')$$

$$\times \exp\left[\frac{ik}{2f}(P_0'^2 - P_0''^2)\right] \times \exp\left[\frac{ik}{2f}(P_1'^2 - P_1''^2)\right]$$
$$\times \exp\left\{-\frac{ik}{f}[(P_0'+P_2')P_1' - (P_0''+P_2'')P_1'']\right\}$$
$$\times \exp\left[\frac{ik}{f}(P_2'^2 - P_2''^2)\right] \exp\left[\frac{ik}{2f}(P_3''^2 - P_3''^2)\right]$$
$$\times \exp\left\{-\frac{ik}{f}[(P_2'+P_4')P_3' - (P_2''+P_4'')P_3'']\right\}$$
$$\times dP_0' dP_0'' dP_1' dP_1'' dP_2' dP_2'' dP_3' dP_3''. \tag{8}$$

After integrating the eq. (8) with respect to P_1', P_1'', P_2', P_2'', P_3', P_3'' and letting $P_4' = P_4''$, the following expressions for the intensity distribution in the Fourier plane is obtained

$$J(P_4) = \frac{1}{\lambda^4 f^4}\iint \Gamma(P_0', P_0'')\hat{A}\left(\frac{P_0'+P_4'}{\lambda f}\right)\hat{A}^*\left(\frac{P_0''+P_4''}{\lambda f}\right) dP_0' dP_0'', \tag{9}$$

where $\hat{A}$ denotes the Fourier transform of the object amplitude transmittance A.

Since for an incoherent light source of intensity distribution $t(P_0')$ the mutual coherence function is equal to

$$\Gamma(P_0', P_0'') = \begin{cases} t(P_0')\,\delta(P_0'-P_0''), & P_0' \in \Sigma_s \\ 0 & P_0' \notin \Sigma_s' \end{cases} \tag{10}$$

where Σ_s is the source area, the diffraction image intensity $J(P_4)$ equals

$$J(P_4) = C\iint \hat{I}_s\left(\frac{P_2'-P_2''}{\lambda f}\right) A(P_2')A^*(P_2'')$$
$$\times \exp\left[-\frac{ik}{f}(P_4'P_2' - P_2''P_4'')\right] dP_2' dP_2''. \tag{11}$$

Here $\hat{I}_s$ is the Fourier transform of the luminance distribution in the source.

In the new variables $V = P_2' - P_2''$, $W = P_2' + P_2''$ the eq. (11) takes the form

$$J(P_4) = C\int \hat{I}_s\left(\frac{V}{\lambda f}\right)\exp\left(-\frac{ik}{f}P_4 V\right)\left[\int A\left(\frac{W+V}{2}\right)A^*\left(\frac{W-V}{2}\right)dW\right]dV. \tag{12}$$

The object spectrum intensity $J(P_4)$ will be determined by the convolution of the Fourier transform of the object auto-correlation with the luminance distribution in the light source. Namely,

$$J(P_4) = C\left[\int \hat{I}_s\left(\frac{V}{\lambda f}\right)\exp\left(-2\pi i\frac{V}{\lambda f}P_4\right)dV\right.$$
$$\left.\otimes\left[\int R_f(V)\exp\left(-2\pi i\frac{V}{\lambda f}P_4\right)dV\right]\right.$$
$$= C\hat{\hat{I}}_s(P_4)\otimes\hat{R}_f\left(\frac{P_4}{\lambda f}\right) = CI_s(P_4)\otimes\hat{R}_f\left(\frac{P_4}{\lambda f}\right), \tag{13}$$

where $R_f(V) = \int A\left(\frac{W+V}{2}\right)A^*\left(\frac{W-V}{2}\right)dW$ is the auto-correlation of the transmittance A. This is a particular case of far-field diffraction, which occurs whenever z_4 tends to infinity. This case is realized in the system, when $z_3 = f_2$, $z_4 = f_2$. Generally, as it was shown in [8], the light intensity distribution in the diffraction image from the plane diffracting aperture illuminated by a partially coherent light beam is proportional to the convolution of the Fourier transform of the stationary part of the mutual intensity in the aperture plane with the light intensity distribution which could appear in the case of coherent illumination of the same aperture by a wave emerging from the centre of a effective incoherent light source giving the same mutual intensity function in the illuminated area*.

Let us assume as an object a set of 2N slits each of width $2a$. The transmittance of such an object is equal to

$$A(x) = \begin{cases} 1 & a(4k-3) \leqslant |x| \leqslant a(4k-1),\ k = 1, 2, \ldots, N \\ 0 & \text{for the others.} \end{cases}$$

Since the position of the slits may be described with the help of the localizing function

$$L(x) = \sum_{k=1}^{N}\{\delta[x-(4k-2)a]+\delta[x+(4k-2)a]\}, \tag{14}$$

* Comp. generalized Schell's theorem [8] which says that

$$J(P_4) = \mathscr{F}\left[\Gamma_2\left(\frac{P_4}{\lambda r_2}\right)\otimes J_0(P_0, P_4)\right.,$$

where

$$\Gamma_2(u) = \int J_s(P_s)\exp\left[-\frac{ik}{r_i}\cos vP_s u\right]dP_s,$$

and r_2 denotes the distance of the diffracting aperture from the observation plane, v — the angle between the direction of illuminating beam incidence and the normal to the diffracting aperture, $J_s(P_s)$ — the light intensity distribution in the surface of effective light source, $J_0(P_0, P_4)$ — light intensity distribution in coherent diffraction image from a light source located at the centre of the effective light source.

while the transmittance of the single slit is equal to

$$A_1(x) = \Pi\left(\frac{x}{a}\right), \tag{15}$$

where Π denotes a rectangular formula, then the transmittance of the object is defined by the convolution

$$A(x) = A_1(x) \otimes L(x). \tag{16}$$

By Fourier-transforming eq. (16) we obtain

$$\hat{A}(\mu) = \hat{A}_1(\mu) \cdot \hat{L}(\mu). \tag{17}$$

Since the transforms of $A(x)$, $L(x)$ are respectively equal to

$$\begin{aligned} \hat{A}_1(\mu) &= \frac{\sin(2\pi\mu a)}{\pi\mu/2}, \\ \hat{L}(\mu) &= 2\sum_{k=1}^{N} \cos[2\pi\mu a(4k-2)], \end{aligned} \tag{18}$$

the transform of the auto-correlation function has the form

$$\hat{R}_t\left(\frac{x}{\lambda f}\right) = \frac{4\sin^2(2\pi ax/\lambda f)}{\pi^2 x^2/\lambda^2 f^2}\left\{\sum_{k=1}^{N} \cos\left[(4k-2)\frac{2\pi ax}{\lambda f}\right]\right\}^2. \tag{19}$$

By taking advantage of (13) and (19) the intensity distribution of the object spectrum may be expressed by the following integral

$$J(x) = \int_{x-\frac{df_2}{f_1}}^{x+\frac{df_2}{f_1}} I_s(z)\sin^2\left(\frac{2\pi az}{\lambda f_2}\right)\frac{1}{z^2}\left\{\sum_{k=1}^{N}\left[\cos\left((4k-2)\frac{2\pi bz}{\lambda f_2}\right)\right]\right\}^2 dz,$$

$$f_1 = z_1, f_2 = z_4. \tag{20}$$

3. The numerical calculations and results

The relation (20) was a basic formula for numerical calculations. We have assumed $\lambda = 628$ nm, and $f_1 = f_2 = f = 200$ mm. The following slit widths $2d$ have been assumed: 0, 160, 320, 480, 640, 800, 960, 1120, and 1440 μm (see figs. 4–7). The respective correlation coefficient defined by the formula

$$\gamma(x) = \operatorname{sinc}\left[\frac{2dx}{\lambda f}\right] \tag{21}$$

is drawn in fig. 2.

Two types of filters were used, the parabolic and Straubel type of $(1-x^2/d^2)^n$ amplitude structure for $n = 1, 2, 4$. The transmittances of those filters with the associated numbering are presented in fig. 3. The

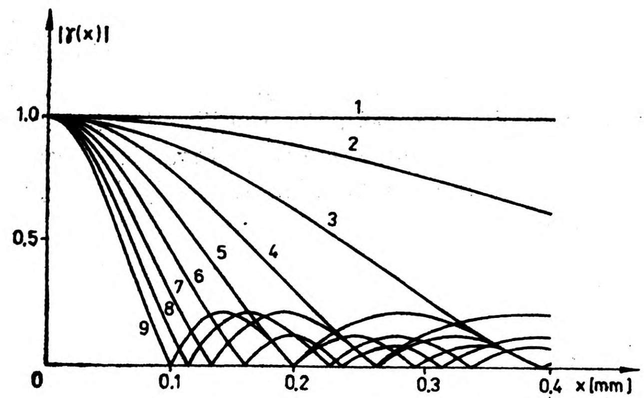

Fig. 2. Dependence of the partial coherence degree γ upon the distance of the points in the light field x for different widths $2d$ of the light sources: 1 — 0 (totally incoherent source), 2 — 160, 3 — 320, 4 — 480, 5 — 640,6 — 800, 7 — 960, 8 — 1120, 9 — 1440μm

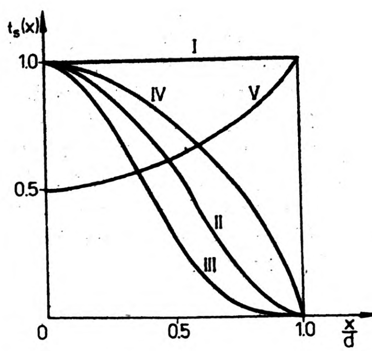

Fig. 3. Filter transmittance:
I $t_s(x) = 1$,
II $t_s(x) = (1-x^2/d^2)^2$,
III $t_s(x) = (1-x^2/d^2)^4$,
IV $t_s(x) = 1-x^2/d^2$,
V $t_s(x) = 0.5(1+x^2/d^2)$

Table. Characteristics of the periodic objects under test

Number of slits	Width of the slit $2a$ [μm]	Distance of the neighbouring slits $2b$ [μm]
2	40	80
2	40	160
4	40	80
4	40	160
10	40	160

characteristic of the examined periodic structures have been given in table.

The light intensity distribution in the object spectrum has been examined for all the combinations of source width, apodiser, and periodic structure. The obtained relative quantities (normalized by the intensity of the main maximum in coherent illumination) are shown in the graphs (figs. 4–7). It follows that (figs. 4a, 5a, 6a, 7a, 8a) with the increasing sizes of the source the contrast is reduced (curves 1–6). For the illumination near the incoherent one (figs. 4a and 6a) even a contrast inversion occurs. An introduction of filters results in a change in position of principal maxima, particularly well visible in fig. 8.

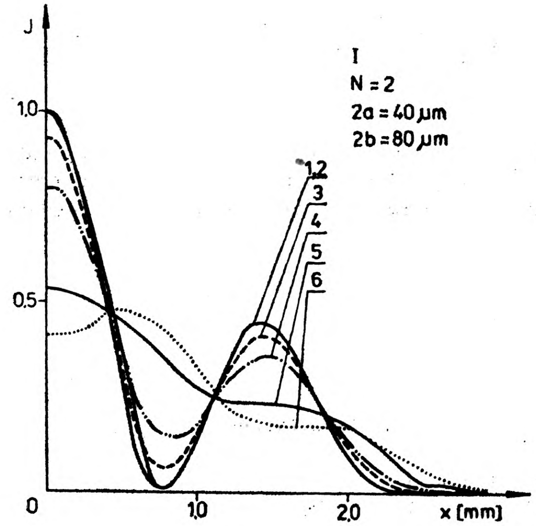

Fig. 4a. Distributions of the light intensities in the diffraction pattern from two slits of the width $2a = 40$ μm, and the distance between the centres $2b = 2 \times 2a = 80$ μm, for filter I and light sources of sizes: 1 — 0, 2 — 160, 3 — 480, 4 — 800, 5 — 1440, and 6 — 1920 μm

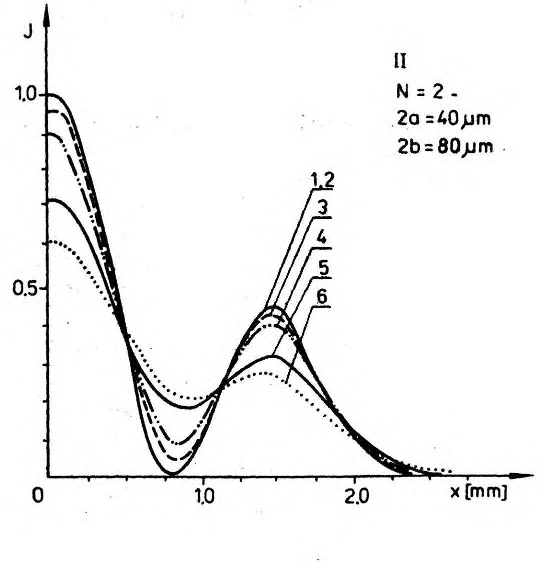

Fig. 4b. The same as in fig. 4a, but for filter II

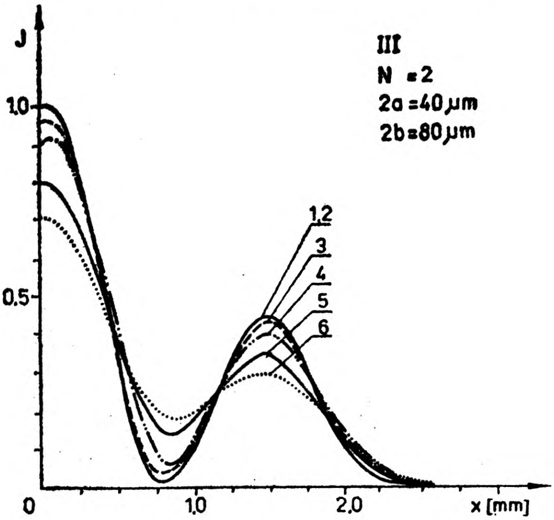

Fig. 4c. The same as in fig. 4a, but for filter III

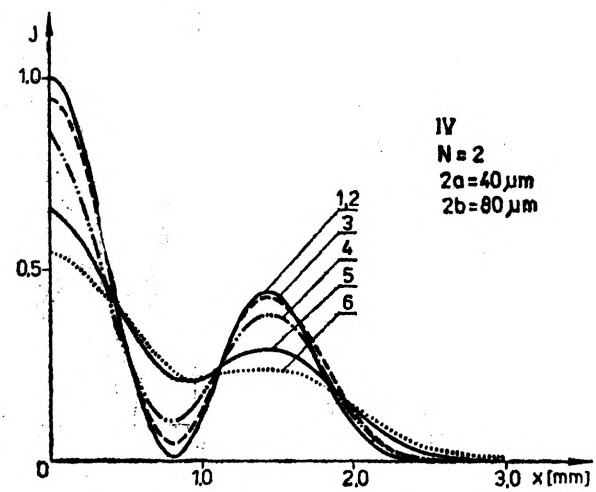

Fig. 4d. The same as in fig. 4a, but for filter IV

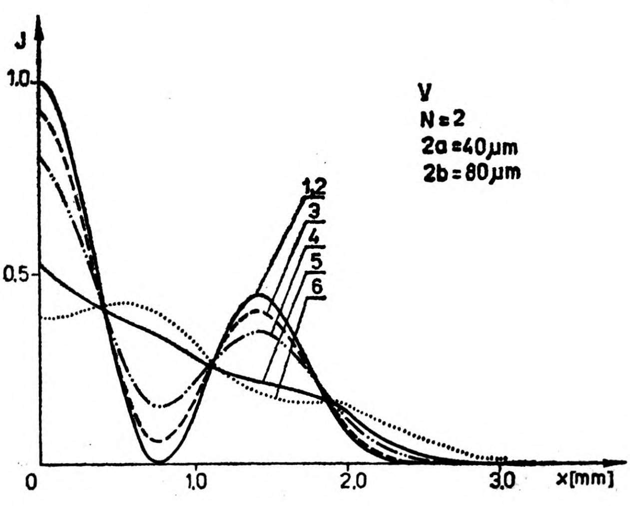

Fig. 4e. The same as in fig. 4a, but for filter V

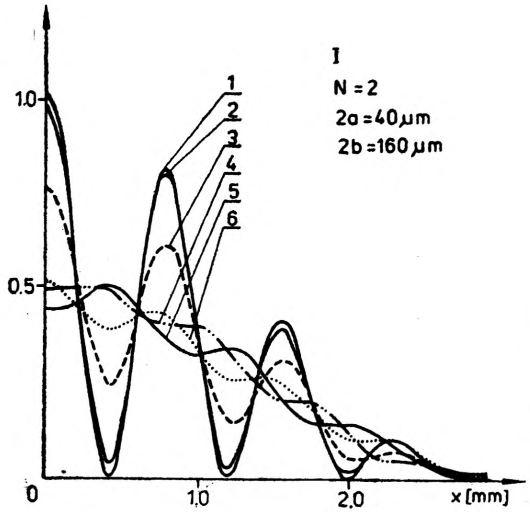

Fig. 5a. Distributions of light intensities in the diffraction pattern from two slits of the width $2a = 40$ μm, and the distance between the centres $2b = 4 \times 2a = 160$ μm for filter I (for the light sources of sizes the same as in fig. 4a)

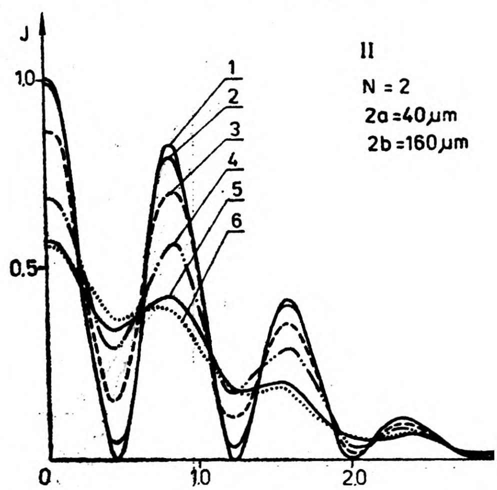

Fig. 5b. The same as in fig. 5a, but for filter II

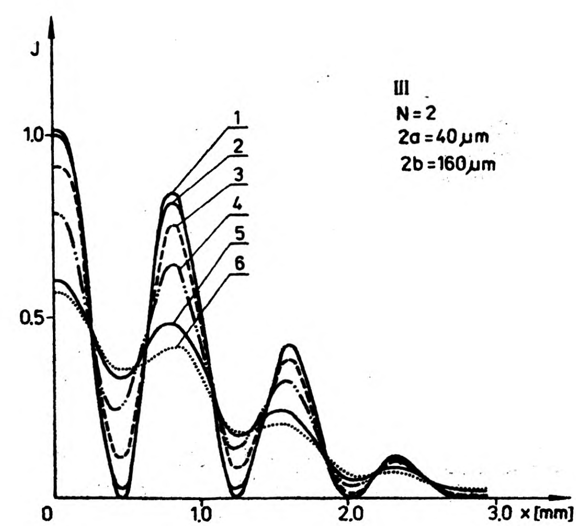

Fig. 5c. The same as in fig. 5a, but for filter III

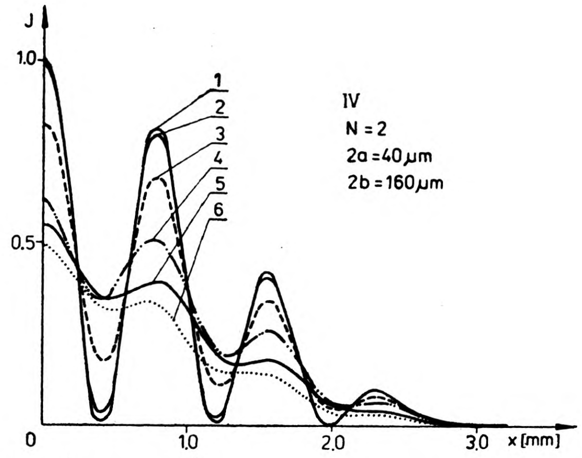

Fig. 5d. The same as in fig. 5a, but for filter IV

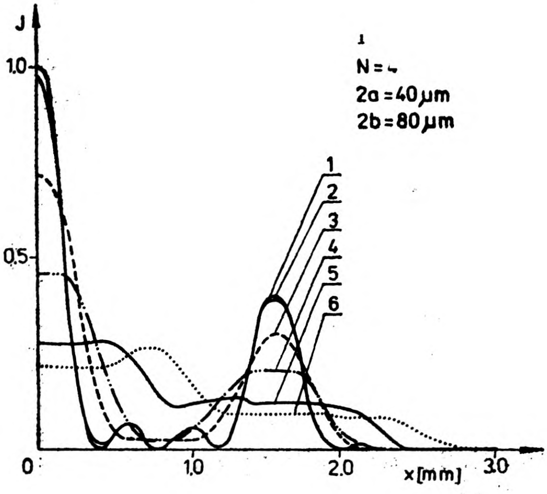

Fig. 6a. Distributions of the light intensities in the diffraction pattern from four slits of the width $2a = 40$ μm and the distance between the centres $2b = 80$ μm for filter I (for the light sources of sizes the same as in fig. 4a)

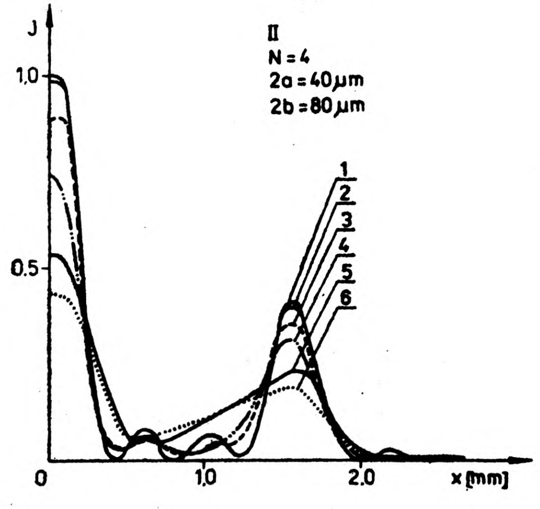

Fig. 6b. The same as in fig. 6a, but for filter II

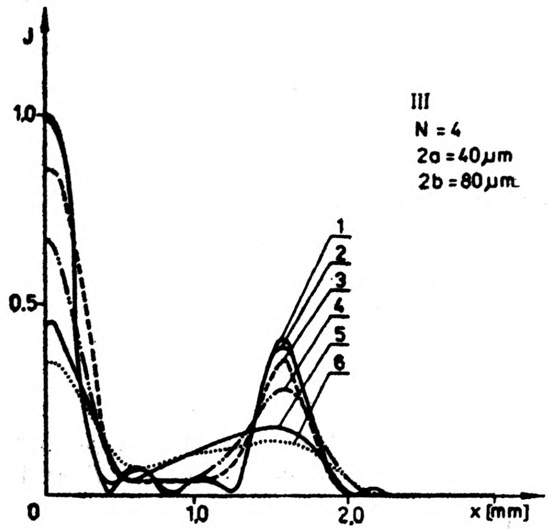

Fig. 6c. The same as in fig. 6a, but for filter III

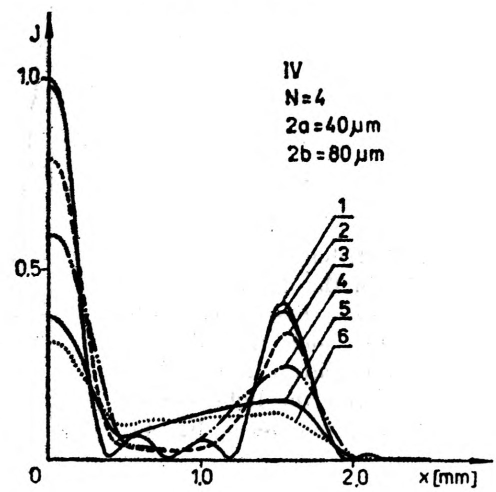

Fig. 6d. The same as in fig. 6a, but for filter IV

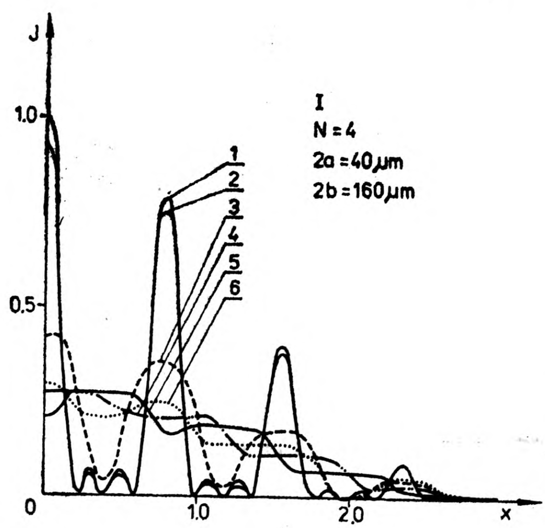

Fig. 7a. Distributions of the light intensities in the diffraction pattern for four slits of the width $2a = 40$ μm and the distance between the centres $2b = 160$ μm for filter I (for the light sources of sizes the same as in fig. 4a)

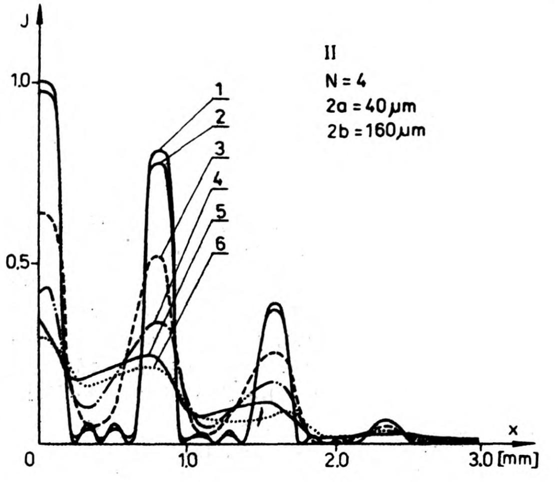

Fig. 7b. The same as in fig. 7a, but for filter II

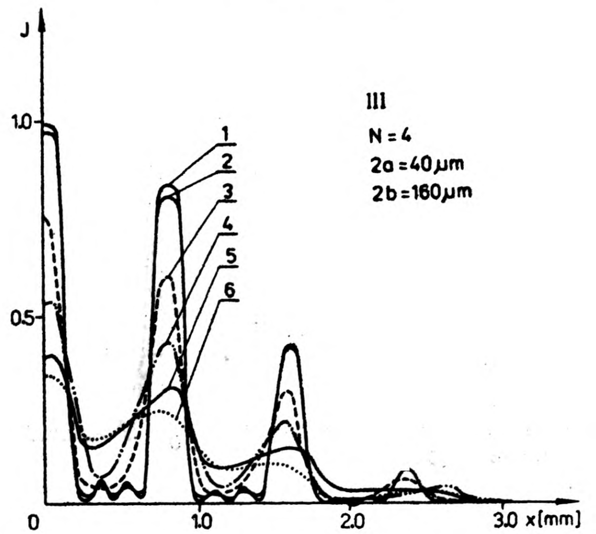

Fig. 7c. The same as in fig. 7a, but for filter III

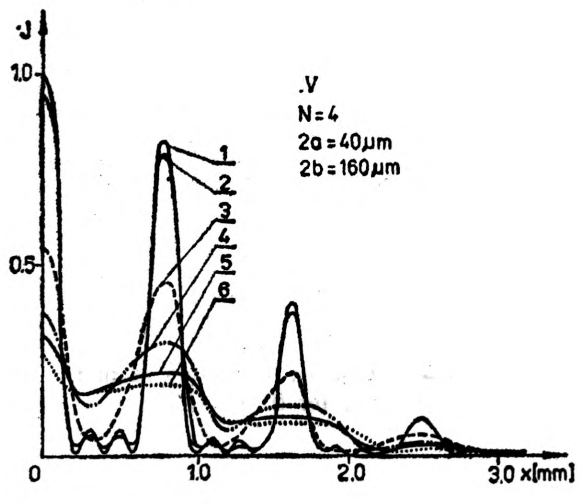

Fig. 7d. The same as in fig. 7a, but for filter IV

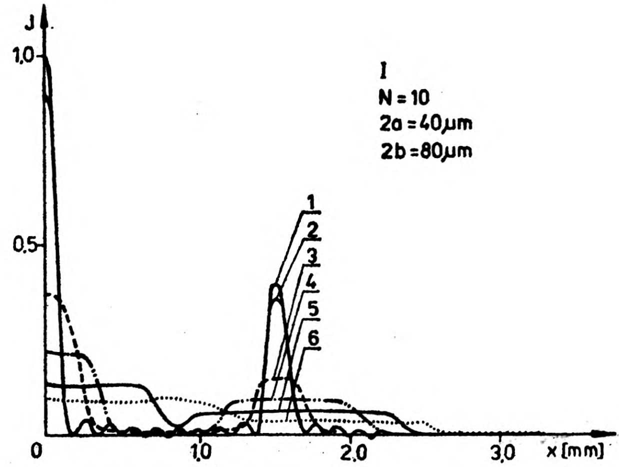

Fig. 8a. Distributions of the light intensities in the diffraction pattern for ten slits of the width $2a = 40$ µm, and the distance between the centres $2b = 80$ µm for filter I (for the light sources of sizes the same as in fig. 4a)

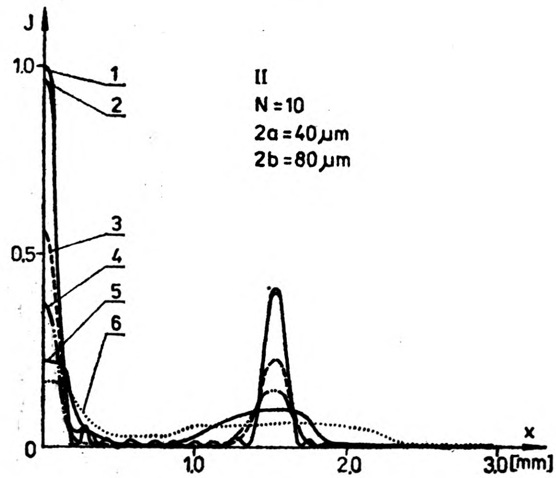

Fig. 8b. The same as in fig. 8a, but for filter II

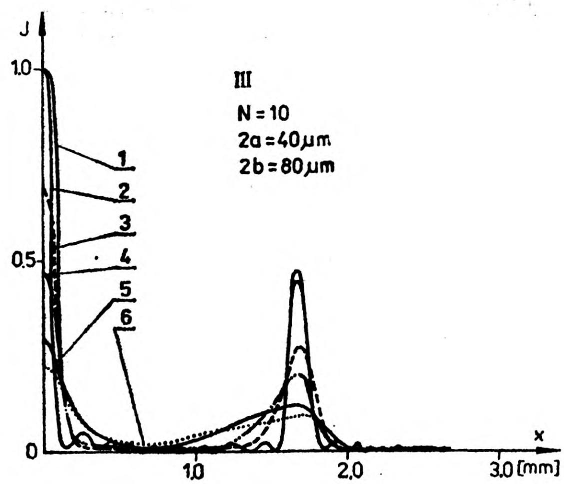

Fig. 8c. The same as in fig. 8a, but for filter III

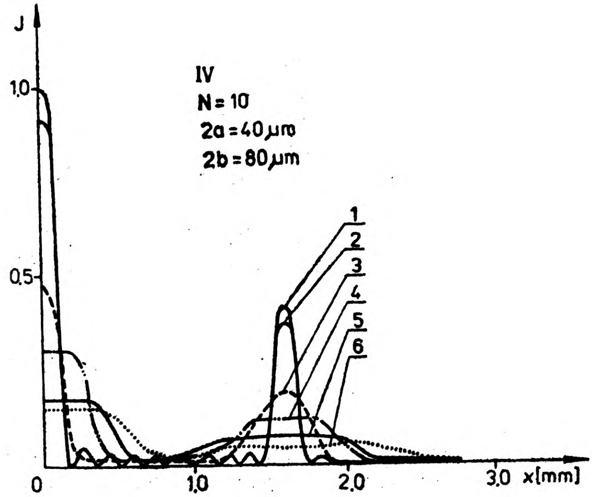

Fig. 8d. The same as in fig. 8a, but for filter IV

The parabolic filter V reduces the contrast for nearly incoherent illumination (fig. 4e, curves 5, 6) but it does not cause any change an intensity spectrum for the nearly-coherent source (curves 1, 2). The filters II, III and IV cause some increase in intensity at the maxima, accompanied by some decrease at the minima (figs. 4bcd, 5bcd). This effect is greater for the illumination closer to incoherent, while the greatest changes occur for the slit widths $2a = 40$ μm and the distances between the centres $2b = 80$ μm when using filter III. When the number of slits increases the filter II gives greater intensity at the maxima in the whole range of illumination intensity (figs. 6bcd, curves 1–6); the intensity being the greater the closer the illumination to an incoherent one (figs. 5ab, 6ab).

The smallest intensity at the secondary maxima is given by the filter II (fig. 6b), while the main maximum becomes narrower. The filter III causes some broadening of the maxima (fig. 6c). When the distances between the slits increase (figs. 7bcd) the filter III gives greater values of intensity with simultaneously broadening of the maxima for nearly coherent illumination, while nearly incoherent illumination results in some narrowing of the same maxima (fig. 7c, curve 3). The results obtained indicate a possibility of a definite modification of the object spectrum by applying the filters of simple transmittances. The experimental results will be published in the next part of this paper.

References

[1] Kumar R., Bhatnagar G. S., Chopra K. N., Atti della Fondazione Giorgio Ronchi **2** (1974), 207.

[2] Maggo J. N., Chopra K. N., Bhatnagar G. S., Optica Acta **12** (1973), 995.

[3] FOREMAN J. W., Jr., HUNT G. H., LAWSON E. K., Appl. Opt. 10 (1971), 105.
[4] MONDAL P. K., SLANSKY S., Optica Acta 10 (1970), 779.
[5] JAISWAL A. K., BHOGRA R. K., Optica Acta 12 (1973), 965.
[6] BORN M., WOLF E., *Principles of Optics*, Pergamon Press, New York 1964.
[7] MAGIERA A., MAGIERA L., PLUTA M., Optik 56 (1980), 413.
[8] ZAJĄC M., Doctor's Thesis, Technical University of Wrocław, Wrocław 1977.

Received December 4, 1979
in revised form June 6, 1980

Расширение объектного спектра одномерных прямоугольных периодических структур в системах с неоднородной освещённой апертурой

Определены распределения интенсивности в дифракционном спектре одномерных периодических объектов. Исследована зависимость дифракционного спектра от распределения освещения источника, а также от свойств объектной структуры. Численный расчёт сделан для всех комбинаций: распределение интенсивности источника, ширина объекта, частота структуры.